

LETTER

Application of high frequency biasing and its effect in STOR-M tokamak

To cite this article: Debyoti Basu *et al* 2020 *Nucl. Fusion* **60** 094001

View the [article online](#) for updates and enhancements.

You may also like

- [Modification of plasma rotation with resonant magnetic perturbations in the STOR-M tokamak](#)
S Elgrw, Y Liu, A Hirose et al.
- [Effects of lithium coating of the chamber wall on the STOR-M tokamak discharges](#)
A. Rohollahi, S. Elgrw, A. Mossman et al.
- [Tangential and Vertical Compact Torus Injection Experiments on the STOR-M Tokamak](#)
Xiao Chijin, D Liu, S Livingstone et al.

Letter

Application of high frequency biasing and its effect in STOR-M tokamak

Debjyoti Basu^{1,2} , Masaru Nakajima¹, A.V. Melnikov^{3,4} , Julio J. Martinell⁵ , David McColl¹, Raj Singh², Chijin Xiao¹  and Akira Hirose¹

¹ Plasma Physics Laboratory, University of Saskatchewan, 116 Science Place, Saskatoon, SK, S7N5E2, Canada

² Present address: Institute for Plasma Research, Bhat, Gandhinagar-382428, India

³ NRC Kurchatov Institute, 123182, Moscow, Russian Federation

⁴ National Research Nuclear University MEPhI, 115409, Moscow, Russian Federation

⁵ Instituto de Ciencias Nucleares-UNAM, Mexico D.F. 04510, Mexico

E-mail: debjyotibasubasu@gmail.com and martinel@nucleares.unam.mx

Received 2 March 2020, revised 10 May 2020

Accepted for publication 19 May 2020

Published 3 August 2020



CrossMark

Abstract

A pulsed oscillating power amplifier has been developed to apply high frequency biasing voltage to an electrode at the edge of the STOR-M tokamak plasma. The power amplifier can deliver a peak-to-peak oscillating voltage ± 60 V and current 30 A within the frequency range 1 kHz–50 kHz. The electrode is located in the equatorial plane at radius $\rho = 0.88$. The frequency of the applied voltage has been varied between discharges. It is observed that the plasma density and soft x-ray intensity from the plasma core region usually increase at lower frequency regime 1 kHz–5 kHz as well as relatively higher frequency regime 20 kHz–25 kHz but seldom increase in between them. Increment of τ_E has been observed 40% and 20% for the frequency regimes of 1 kHz–5 kHz and 20 kHz–25 kHz, respectively, and τ_p increment is 25% for both frequency regimes. Transport simulation has been carried out using the ASTRA simulation code for STOR-M tokamak parameters to understand the physical process behind experimental observations at the higher frequency branch. The model is based on geodesic acoustic mode (GAM) excitation at resonance frequency associated with Ware-pinch due to the oscillating electric field produced by biasing voltage, which can suppress anomalous transport. Simulation results reproduce the experimental trends quite well in terms of the density, particle confinement, as well as energy confinement time evolution. All the results indicate that high frequency biasing is capable of improving confinement efficiently.

Keywords: ac electrode biasing in ‘kHz’ range in STOR-M tokamak, particle and energy confinement time increases, clearly two frequency regimes 1 kHz–5 kHz and 20 kHz–25 kHz shows confinement increment

(Some figures may appear in colour only in the online journal)

Edge plasma turbulence in tokamaks play a crucial role in plasma transport and confinement [1]. In general, it is believed that anomalous transport in tokamaks is governed by plasma turbulence. Experimentally, it has been established that anomalous transport happens mostly due to edge electrostatic turbulence [2, 3], but the basic mechanism of edge turbulence has not been clear until now. An interesting feature of

turbulence phenomena is the possibility to drive zonal flows and geodesic acoustic mode (GAM) [4, 5] when it reaches a certain energy level and may help to trigger H-mode in a tokamak. Turbulence has an interesting nature and is of great importance in relation to tokamak plasma confinement where it generally worsens plasma confinement, though sometimes deterioration is reduced, leading to relatively better plasma

confinement. Therefore, high frequency biasing [6] may be another approach to understanding the role of turbulence in plasma confinement.

Previously, a series of dc and low frequency (around a few hertz) ac electrode biasing [7–12] and turbulent feedback experiments [13–15] have been performed to understand the nature of anomalous transport and improved confinement achieved by edge turbulence suppression. Recently, it was planned to perform high frequency (kilo-Hertz range), electrode biasing experiments on the STOR-M tokamak to study the dependency of transport on biasing voltage frequency. So, an ac broadband (1 kHz–50 kHz) power amplifier has been developed to meet the experimental needs to amplify a broadband signal without phase shift.

In this paper, a brief description of the power amplifier development, the experimental results and the analysis of its physical nature through transport simulation using the ASTRA code will be discussed.

The STOR-M tokamak is a limiter-based small tokamak with circular plasma cross-section having major and minor radii of 46 cm and 12 cm, respectively. In high-frequency biasing experiments, an oscillating voltage of ± 60 V has been applied by the developed power amplifier at the plasma edge through an electrode made of rectangular stainless steel plates located in the equatorial plane at a plasma radius of $10.5(\rho = 0.88)$ cm. The frequency of the applied voltage was varied from 1 kHz to 25 kHz on a shot to shot basis in this experiment, based on previous frequency scanning results where they showed that there were very rare changes of density as well as H_α intensity compared with cases without bias above 25 kHz. A 12 channel pin-hole soft x-ray camera masked by a $1.8 \mu\text{m}$ aluminum foil and viewed from a top port [16] was used to measure line-integrated soft x-ray emission intensity. A half-meter monochromator for H_α recording and a 4mm microwave interferometer for line averaged electron density measurement was used.

The power amplifier can deliver an output signal with peak voltage ± 60 V and maximum current 30 A without any distortion in any waveform within the frequency range 1 kHz–50 kHz when its input voltage and current are 0.25 V and 0.5 A, respectively. The selected frequency range has been chosen based on the dominant frequency of the drift mode driven by density gradients present in STOR-M. The power amplifier has two key parts which amplify voltage (figure 1) and current (figure 2) and thus the overall power of a waveform. Voltage amplification was carried out through a high frequency and power MOSFET op-amp PA340CC. The voltage was amplified by two inverting op-amp amplifiers with a resultant amplification factor of around 175. MJH11021 PNP and MJH11022 NPN darlington pairs with ratings 250 V and 10 A were used for current amplification. Nine identical push-pull amplifiers were connected in parallel to deliver the combined high power required for the experiments. A voltage divider and a 0.1Ω sampling resistor were used to monitor electrode voltage and current through the plasma. The power amplifier is gated and driven by a function generator. The activation and operational time duration of the amplifier is controlled by a pulsed controller circuit using solid state analog switch

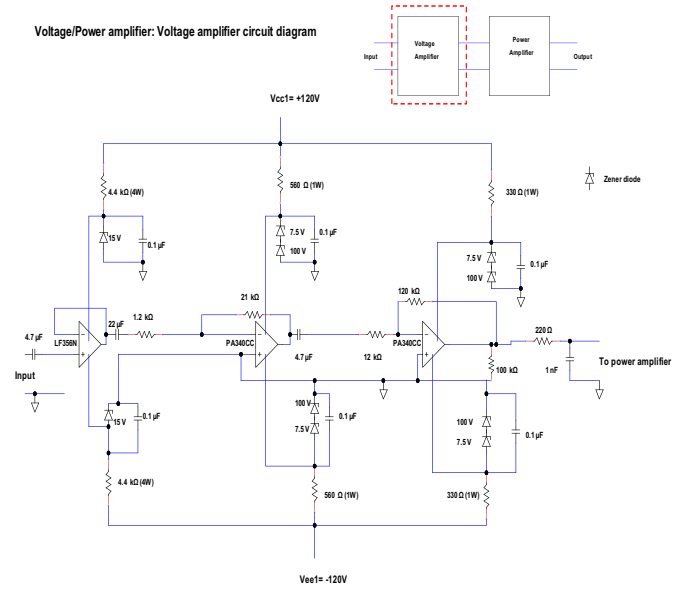


Figure 1. Voltage amplifier section.

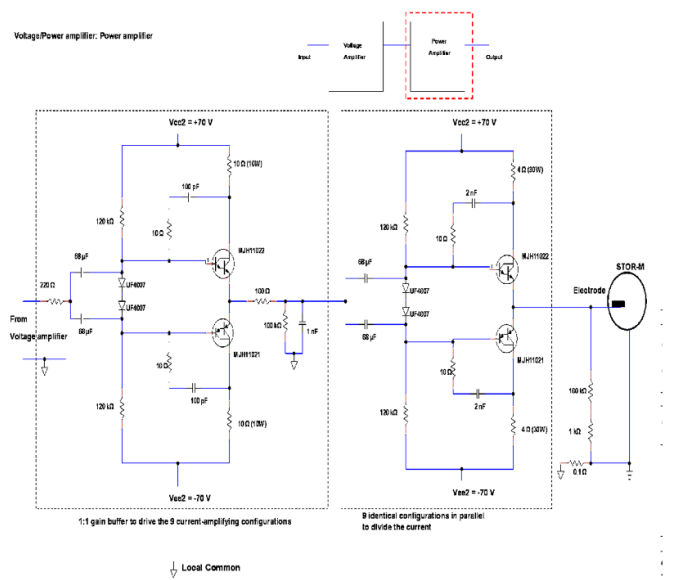


Figure 2. Current amplifier section.

LF13202. The pulsed controller circuit is turned on by a master optical trigger pulse. Pulse delay and its width can be varied from 0.5 ms–44 ms and 1 ms–45 ms, respectively.

The frequency was varied between shots from 1 kHz to 25 kHz. Interestingly, biasing improves confinement for frequency regimes of 1 kHz–5 kHz and 20 kHz–25 kHz. The confinement rarely improved outside these two frequency regimes. A typical plasma shot with and without biasing is shown in figure 3.

In this typical example, a triangular voltage signal with peak to peak voltage of ± 60 V was applied from 10 ms to 21 ms at 5 kHz and 25 kHz during the plateau of the STOR-M discharge current as shown in figure 3. An important feature is that the overall plasma density has increased without a significant change in H_α intensity, as shown in figures 3(d)

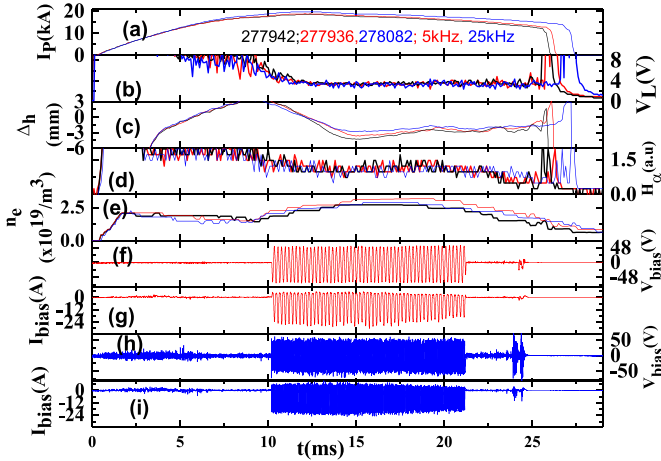


Figure 3. Temporal evolution of plasma parameters without (black line) and with (red line 5 kHz and blue line 22 kHz) biasing (a) plasma current, (b) loop voltage, (c) plasma horizontal position, (d) Plasma H_α intensity, (e) line averaged density, (f) bias voltage, (g) bias current at low frequency; (h) bias voltage, (i) bias current at high frequency.

and (e). Horizontal equilibrium plasma position started to shift during application of the high frequency bias voltage but came back to its equilibrium position due to the position feedback control, as seen in figure 3(c). Interestingly, figures 3(f)–(i) show that the maximal value of the electrode current decreases with time while the electrode voltage remains unchanged, indicating improved confinement [7, 17].

Time evolution of the central soft x-ray channel signal and the particle confinement time (τ_p) with and without biasing are presented in figures 4(a) and (b). τ_p is the ratio of electron density n_e to H_α intensity [18], which is enhanced due to biasing. Increments of soft x-ray signals from the central and its adjacent channels have been noticed from the radial profile in the presence of biasing in the time window of 15.5 ms–16.5 ms, as shown in figure 4(c).

These results indicate that an improvement of core plasma confinement may happen due to biasing. The nature of density variation and soft x-ray behaviour at different frequencies is shown in figure 5. Interestingly, it is observed in figures 5(a) and (b) that changes are sometimes opposite in soft x-ray and density time profiles with different bias frequencies. If density is lower at lower frequencies then soft x-ray intensity is higher at lower frequencies compared to that at higher frequencies. In this typical example, density and soft x-ray profiles at 3 kHz, 20 kHz and no bias are compared. To quantify the differences, a percentage increment of $n_e \cdot T_e$ (a.u) has been derived within 15.5 ms–18.5 ms at lower frequencies (1 kHz–5 kHz) as well as in higher frequencies (20 kHz–25 kHz) where the maximum change happened for both profiles. Soft x-ray intensity has been used for the derivation of percentage increment of $n_e \cdot T_e$ (a.u) assuming that it is all due to bremsstrahlung radiation. This radiation, which is received by soft x-ray detectors, can be written as $I_{br} = cn_e^2 T_e^{1/2} Z_{eff}$ [19], where, I_{br} , n_e and T_e are in watt m^{-3} , m^{-3} and eV, respectively, and ‘ Z_{eff} ’ is

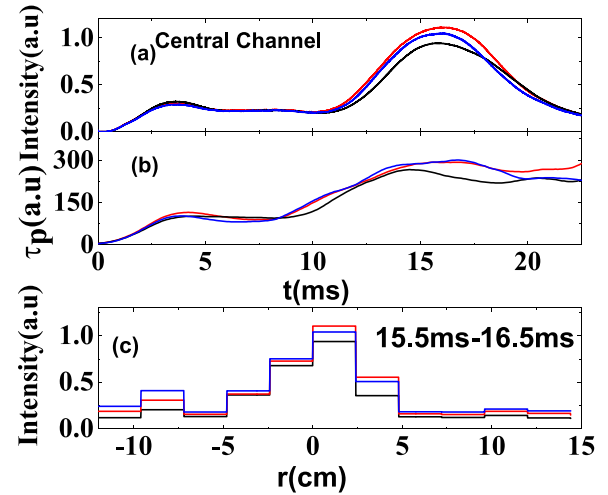


Figure 4. Temporal evolution of (a) soft x-ray central channel, (b) representation of particle confinement time, (c) radial profile of soft x-rays intensity averaged over 15.5 ms–16.5 ms with (red line 5 kHz and blue line 22 kHz) and without (black line) bias.

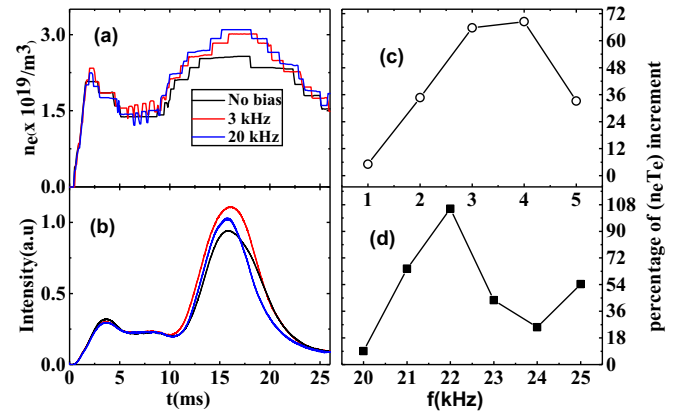


Figure 5. Temporal evolution of (a) density, (b) soft x-ray central channel at without bias (black), with 3 kHz (red) and 20 kHz (blue) bias, frequency dependence of percentage increment of $n_e \cdot T_e$ at (c) lower frequency branch, (d) higher frequency branch.

the effective ion charge state. Here, it is considered that ‘ Z_{eff} ’ remains unaltered in both situations for different frequencies because comparisons between the cases with and without bias show that I_p does not decrease and V_L and H_α do not increase. As a good approximation, it can be concluded that $n_e \cdot T_e \propto I_{br}^2 / n_e^3$.

Smoothed signals of V_L and H_α using adjacent averaging of 25 points have been plotted in figures 6(a) and (b) within the time window of 12 ms–24 ms. V_L and H_α profiles within 15.5 ms–18.5 ms clearly show that they are decreased with biasing. Intensity coming from the same soft x-ray channel has been compared for the cases with and without bias. Since soft x-ray radiation comes from around the plasma center, density value from interferometer data is used for getting a crude approximation. Here, percentage increment of a physical quantity ‘ α ’ is defined as $\frac{\alpha_{with\ bias} - \alpha_{without\ bias}}{\alpha_{without\ bias}} \times 100$. Energy percentage increment reaches its maximum at 4 kHz and 22

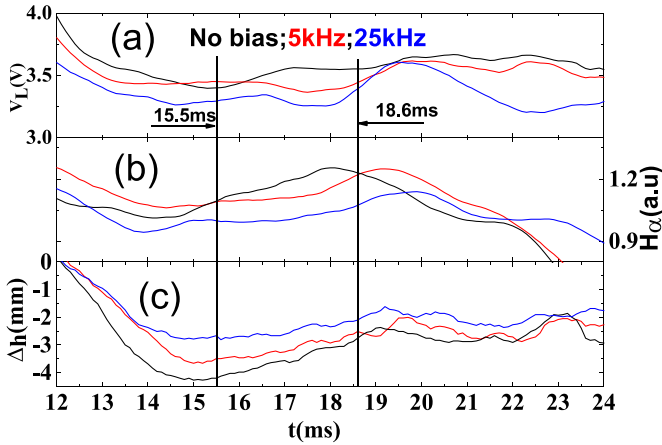


Figure 6. Temporal evolution of zoomed (a) loop voltage (smoothed 25 points), (b) H_{α} -intensity (smoothed 25 points), (c) horizontal position (Δh) at without bias (black), with 5 kHz (red) and 25 kHz (blue) bias.

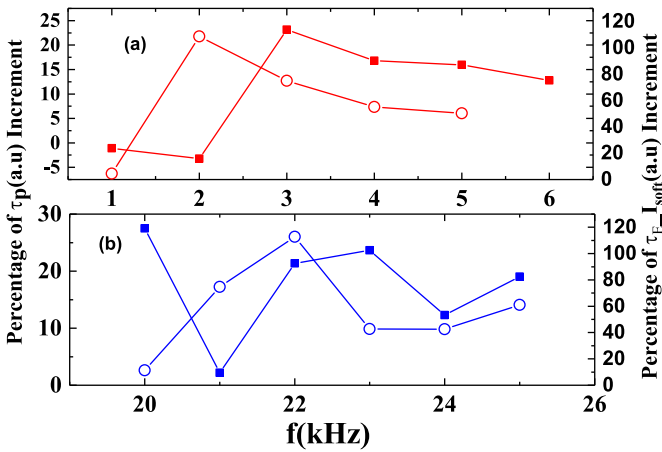


Figure 7. Percentage increment of τ_p (solid square box) and τ_E (hollow circle) (a) lower frequency branch (red line), (b) higher frequency branch (blue line).

kHz, as shown in figures 5(c) and (d). The increment of $n_e T_e$ is an indication of plasma beta enhancement which is supported by Grad–Shafranov shifting of plasma column horizontally from its equilibrium position, as shown in figure 6(c).

Percentage increment of τ_p and a new physical quantity τ_{E_Isoft} are shown in figures 7(a) and (b) for lower and higher frequency regimes, respectively, where $\tau_{E_Isoft} \propto \frac{I_{br}^2}{n_e^3 I_p V_L}$ and $\tau_p \propto \frac{n_e}{H\alpha}$. It is noticed that the shape of frequency profiles of τ_p and τ_{E_Isoft} look almost the same in the lower frequency branch as well as in the higher frequency branch.

τ_E has also been derived from $\tau_{E_kinetic} \approx \frac{\langle n_e \rangle \langle T_e \rangle \langle v_{plasma} \rangle}{I_p V_L}$. The percentage increment of τ_{E_Isoft} and $\tau_{E_kinetic}$ have been plotted in figures 8(a) and (b) for lower and higher frequency regimes, respectively. Interestingly, the frequency profiles of τ_{E_Isoft} and $\tau_{E_kinetic}$ increments at low frequency regime look the same and have the peak value at the same frequency (2 kHz). On the other hand, the frequency profile of the $\tau_{E_kinetic}$ increment is oscillatory in the high frequency regime, which is

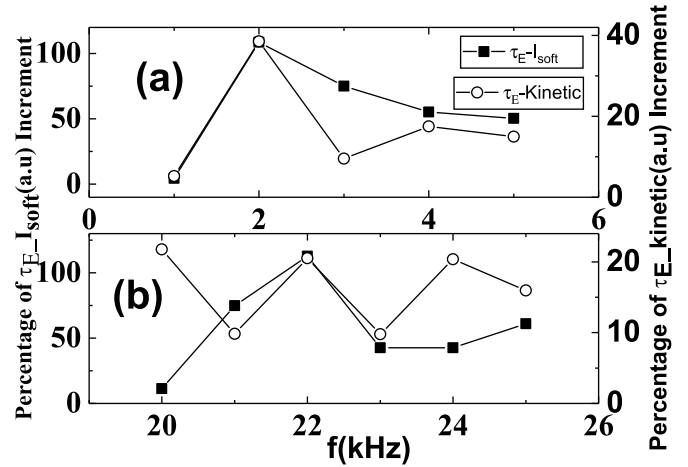


Figure 8. Comparison between percentage increment of τ_{E_Isoft} (solid square box) and $\tau_{E_kinetic}$ (hollow circle) (a) lower frequency branch, (b) higher frequency branch.

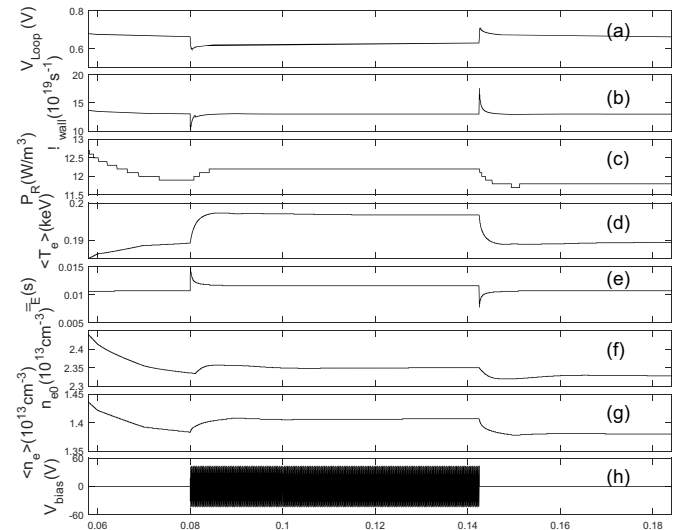


Figure 9. Simulation time evolution of STOR-M discharge of (a) loop voltage, (b) particle flux to wall, (c) radiated power, (d) average electron temperature, (e) energy confinement time, (f) central plasma density, (g) average plasma density, (h) high frequency ac bias voltage of 22 kHz.

unlike the τ_{E_Isoft} increment frequency profile, as clearly seen in figure 8(b). It needs to be mentioned that energy confinement time calculations from $\tau_{E_kinetic}$ (conventional method) and τ_{E_Isoft} (new definition) predict the same frequency peak but their magnitudes differ by a factors of 3–5 times. The factor of difference arises probably due to different causes such as (1) the soft x-ray emission includes not only bremsstrahlung radiation, as it was assumed, but also some contributions from line radiation and (2) τ_{E_Isoft} is more a local measurement around central plasma region while $\tau_{E_kinetic}$ is a plasma volume averaged quantity.

In order to understand the inherent physics of improved confinement, possible mechanisms related to the effect of

ac biased electrodes have been explored. Since the exciting frequency of the applied electric potential remains in the ‘kHz’ range, the formation of a zero frequency zonal flow or other mechanisms like a ponderomotive force [22] effective at ICR frequencies, which may stabilize turbulent modes are not applicable. A possible candidate in the relevant frequency range is GAM which can be driven through resonance from oscillating external currents [6, 20] that create time dependent poloidal flow shear. This produces turbulence suppression by the stochastic Doppler shift due to chaotic stretching of eddies [4]. Accordingly, the fluctuation level is reduced by a factor of $(1 + \tau_c \tau_{c,G} \langle k_\theta \tilde{V}_G^2 \rangle)^{-1}$ which also applies for turbulent diffusion coefficient. It is then plausible to expect that high frequency biasing can excite GAM which does not damp as it would if not resonantly excited and produce some sort of transport barrier that improves confinement. The idea was tested doing a simulation of the plasma evolution using ‘ASTRA’ transport code [21] with the modified turbulent transport coefficients. It has been run using parameters of the STOR-M tokamak in Ohmic heating regime where transport coefficients contain neoclassical as well as turbulent components. Drift wave turbulence can be affected by the high-frequency biasing potential as described above. A resonant electric field is produced by the electrode confined in a small radial region where turbulence reduction takes place. This would be effective when the driving frequency matches the GAM frequency in this edge region of STOR-M which is of the order of $f_{\text{GAM}} \sim c_s/R \sim 22$ kHz when $T_e \sim 40$ eV. The radial electric field is of the order of $E_r \sim V/\Delta_r \sim 6000$ V m⁻¹. A potential variation scale length of $\Delta_r \sim 1$ cm was taken and the reduced anomalous diffusion coefficient for STOR-M is given by [4]

$$D = D_0 \left(1 + 0.0012 E_r^{2/3} f_G \right)^{-1} \quad (1)$$

where D_0 is the diffusion coefficient in the absence of oscillating field and $f_G = \tau_c/\tau_{c,G}$, the ratio of correlation times for fluctuations and GAM. Here, $\tau_c = k_\perp^{-2/3} D^{-1/3} S_v^{2/3}$ was taken, with k_\perp the radial mode extension assumed as 1 cm, $S_v \sim V/\Delta_r^2 B \sim 10^6$ s⁻¹ the velocity shear. The equilibrium diffusion coefficient is estimated as $D \sim 1$ m² s⁻¹. The parameter f_G is not known and is taken in the range 1–5. However, the GAM effect alone is not able to reproduce the complete phenomena, so another effect was included. This may come from an increased pinch velocity that confines particles against diffusion. Electrons traveling toroidally parallel to the magnetic field can be thrust by the electrode voltage every time when they pass through its region if the transit time matches the ac bias frequency. This allows the electrons to build a toroidal current which can give rise to a Ware-like radial pinch. It turns out that the electron toroidal rotation frequency for the drag velocity corresponding to the edge collisionality, $f_{tr} = eE/2\pi R m_e \nu_{ce}$, has a value ~ 20 kHz, matching the high frequency branch.

Both GAM and radial pinch are resonantly driven by ac voltage, the former producing turbulence and transport

reduction while the later advects particles to the center. GAM is due to the oscillating radial electric field at the electrode that produces oscillating poloidal flow which reaches steady state at the driving frequency. As a result, a transport barrier is formed around the electrode.

These elements were incorporated in transport simulations considering different conditions for f_G . The results having a better agreement with experimental data correspond to choosing $f_G = 3$ for particle diffusion while $f_G = 5$ for thermal diffusivity. In this case there is an improvement of plasma confinement in the density while the electron temperature profile becomes less peaked. The results can be seen in figure 9, for a simulation in which the Ware pinch is increased by 12% during bias. The simulations started by running the code without ac biasing until steady state was reached, having plasma parameters in agreement with typical STOR-M values and then the biasing was turned on. The evolution of representative plasma parameters given by ASTRA simulation can be observed in which the high-frequency potential of 22 kHz with 60 V is applied at time 0.08 s. It is clear that the behavior agrees in general terms with the discharge shown in figure 3. The average electron temperature $\langle T_e \rangle$, radiated power from bremsstrahlung which would be detected in soft x-rays, average and central densities $\langle n_e \rangle, n_{e0}$ and τ_E are increased. Interestingly, particle flux to the wall which would be related to the H_α emission, shows very small changes which also agrees with the experimental outcomes. All these trends from simulation support the scenario of transport reduction by mode stabilization due to resonantly excited GAM associated with high-frequency biasing potential.

According to our knowledge, this is the first time experimental studies of high frequency biasing in ‘kHz’ range have been performed in a tokamak. Previously, elaborate experimental studies of dc biasing through electrode and limiter [11, 23] were performed in STOR-M. Those experiments show that improved confinement happens at +150 V and -350 V with electrode current ~ 22 A. The present high frequency biasing experiments show that improved confinement can be achieved with a triangular pulse of ± 60 V with bias current from -24 A to +2 A at 1 kHz–5 kHz and 20 kHz–25 kHz frequency regimes. The kinetic τ_E increases by 40% and 20% for lower and higher frequency branches, respectively. τ_p is also enhanced around 25% in both frequency regimes. Also, soft x-ray emission is enhanced in the central part of the plasma column, an indication of central energy density enhancement. The simulation of the proposed model also shows same trend of observed results at higher frequency regimes (20–25) kHz. So, a physical explanation for improved confinement at higher frequency regimes may be due to resonant GAM excitation combined with a radial (Ware) pinch produced by the toroidal transit electron current resonantly driven at the bias frequency around 22 kHz. In this experiment, fluctuation studies and flow measurements have not been carried out and remains an important future study for further clarification of the physical mechanism and its simulation modeling for the improved confinement.

Acknowledgments

We would like to acknowledge NSERC for supporting this work. We also would like to acknowledge the machine workshop in our Physics Department. Special thanks go to Mr Chomyshen and Mr Toporowski in the machine workshop for their kind help and friendly approach when needed. The work of A.V. Melnikov was supported by Russian Science Foundation, Project No. 19-12-00312 and in part by the Competitiveness Programme of the National Research Nuclear University 'MEPhI'. JJM was supported by projects PAPIIT IN112118 and Conacyt A1-S-24157.

ORCID iDs

Debjyoti Basu  <https://orcid.org/0000-0002-6489-9284>
 A.V. Melnikov  <https://orcid.org/0000-0001-6878-7493>
 Julio J. Martinell  <https://orcid.org/0000-0002-2728-220X>
 Chijin Xiao  <https://orcid.org/0000-0002-1024-6253>

References

- [1] Van Oost G. et al 2003 *Plasma Phys. Control. Fusion* **45** 621
- [2] Ritz C. and Bengtson R.D. et al 1984 *Phys. Fluids* **27** 2956
- [3] Liewer P.C. and McChesney J.M. et al 1986 *Phys. Fluids* **29** 309
- [4] Diamond P.H. et al 2005 *Plasma Phys. Control Fusion* **47** R35
- [5] Basu D. et al 2018 *Nucl. Fusion* **58** 024001
- [6] Shurygin R.V. and Melnikov A.V. 2018 *Plasma Physics Reports* **44** 303
- [7] Taylor R.J. et al 1989 *Phys. Rev. Letter* **63** 2365
- [8] Weynants R.R. et al 1992 *Nucl. Fusion* **32** 837
- [9] Basu D. et al 2012 *Phys. Plasmas* **19** 072510
- [10] Melnikov A.V. et al 2004 *Fusion Science and Technology* **46** 299
- [11] Xiao C. et al 1994 *Phys. Plasmas* **1** 2291
- [12] Silva C. et al 2004 *Plasma Phys. Control. Fusion* **46** 163
- [13] Kan Z. et al 1997 *Phys. Rev. E* **55** 3431
- [14] UCKAN T. et al 1995 *Nucl. Fusion* **35** 487
- [15] Brooks J.W. et al 2019 *Rev. Sci. Instrum.* **90** 023503
- [16] Xiao C. et al 2008 *Rev. Sci. Instrum.* **79** 10E926
- [17] Heikkinen J.A. 2001 *Phys. Plasmas* **8** 2824
- [18] Hidalgo C. et al 2004 *Plasma Phys. Control. Fusion* **46** 287
- [19] Silver E.H. et al 1982 *Rev. Sci. Instrum.* **53** 1198
- [20] Hung C.P. and Hassam A.B. 2013 *Phys. Plasmas* **20** 092107
- [21] Pereverzev G.V. and Yushmanov P.N. 2002 *Astra: Automated System for Transport Analysis (Max-Planck-Institute für Plasmaphysik Rep IPP 5/98)* (Garching: IPP) (https://w3.pppl.gov/~hammett/work/2009/Astra_ocr.pdf)
- [22] Martinell J.J. et al 2013 *Radiat. Eff. Defects Solids* **168** 866
- [23] Zhang W. et al 1992 *Phys. Fluids B* **4** 3277